Supplementary Information

Cooperative and competitive effects in pH-dependent surface composition of atmospherically relevant organic ions in water

Ricardo R. T. Marinho[a,b], Olle Björneholm[c], Alexandra Mocellin[a], Anderson Herbert de Abreu Gomes[b,d], Gunnar Öhrwall[e], Oscar Cardoso Araújo[a], Túlio C. R. Rocha[d], Arnaldo Naves de Brito[f]

[a] Institute of Physics. Brasília University (UnB). Box 4455. Brasília 70910-970. Brazil
[b]Institute of Physics, Federal University of Bahia, 40.170-115, Salvador, BA, Brazil
[c]Department of Physics and Astronomy. Uppsala University. P.O. Box 516. 751 20 Uppsala. Sweden
[d]Laboratório Nacional de Luz Síncrotron – LNLS/CNPEM. Caixa Postal 6192. CEP 13083-970. Campinas SP. Brazil
[e-d]MAX IV Laboratory. Lund University. P.O. Box 118. SE-221 00 Lund. Sweden

[f]Institute of Physics Gleb Wataghin, University of Campinas. 13083-859 Campinas -SP. Brazil

7.1. Langmuir Curves

Aqueous solutions containing hydrophobic functional groups may establish a solute monolayer upon reaching a critical concentration. I. Langmuir [1] presented the inaugural model for the adsorption of gases or vapors into solid substrates. The modified model elucidates the process by which solute monolayers form on the surface of the liquid [2-4].

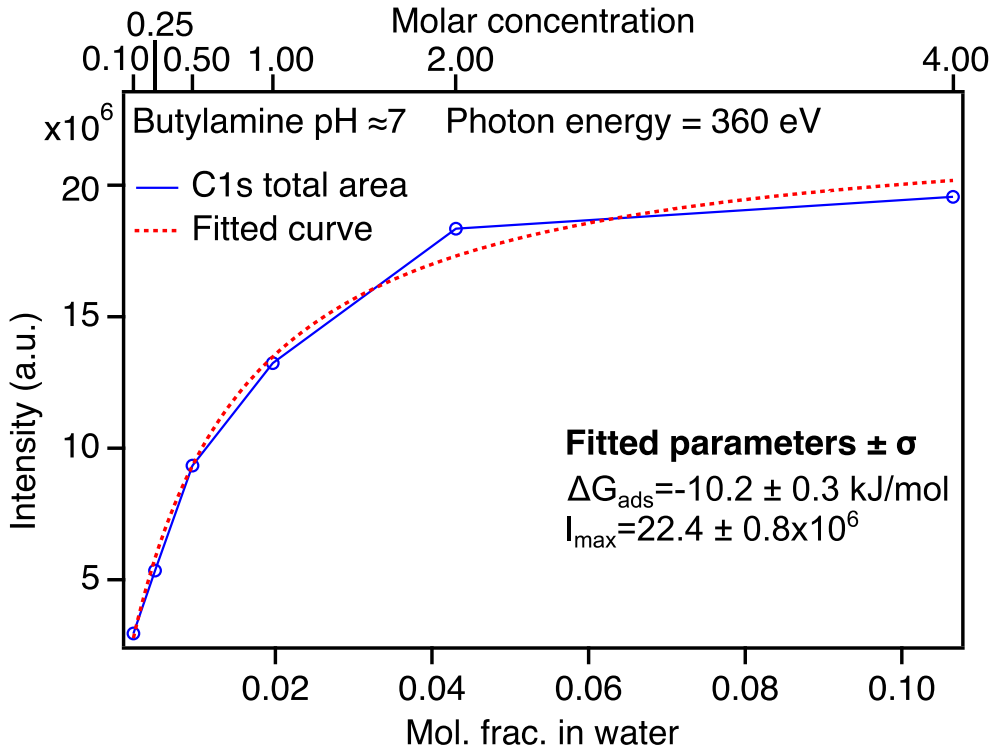

Figure 01: Butylamine C 1s total area at different concentrations at pH ≈ 7 and the fitted modified Langmuir curve as a hatched line. The optimized fitted parameters are also presented. See the text for more details.

Fig. 01 shows the total area of the XPS C 1s spectra of butylamine at pH 7 as a function of the molar fraction (concentration) of the solute in water at the lower (upper) horizontal axis. We fitted the experimental data using the modified Langmuir adsorption model [2]:

$$I(x) = \frac{I_{max} x}{x + (1 - x) * e^{\Delta G_{ads}/k_B T}} \quad (1).$$

In eq. 1, $I(x)$ is the XPS total area intensity for a given molar fraction, concentration, I_{max} is the XPS C 1s total area intensity at full surface coverage situation, x is the solute molar fraction in water, ΔG_{ads} is the adsorption Gibbs free energy in J/mol, k_B is the Boltzmann constant, and T is the sample temperature in Kelvin. We used 10 ºC for the sample temperature at the microjet position where the studied photoelectrons are ejected [5].

A crucial parameter influencing the activation of cloud droplets is surface tension, which can be correlated with the change in Gibbs free energy per molecule necessary to reduce the surface free energy (i.e., the surface tension). ΔG_{ads} per molecule is calculated by dividing the ΔG_{ads} by Avogadro's number N_A. In transitioning from adsorption free-energy to surface tension, we posit that the change in free energy per molecule is wholly consumed in the generation (or reduction) of the interfacial energy across the molecular area, A_m that is occupied. Therefore, the subsequent expression is derived:

$$\gamma = -\frac{\Delta G_{ads}/N_A}{A_m} \quad (2).$$

For small alkylamines like butylamine, the literature values typically fall within the range of 0.3–0.4 nm² per molecule $\approx 0.35\ nm^2$ [6].

Therefore, inserting the numbers we have:

$$\gamma = 48 \pm 2\ mN/m \quad (3).$$

Several standard references report on surface-tension data for organic compounds in aqueous solution (including small amines such as butylamine) that support values in the 40–50 mN/m[7 8 9]

For comparative purposes, it is noteworthy that the surface tension of pure water is roughly 72 mN/m.

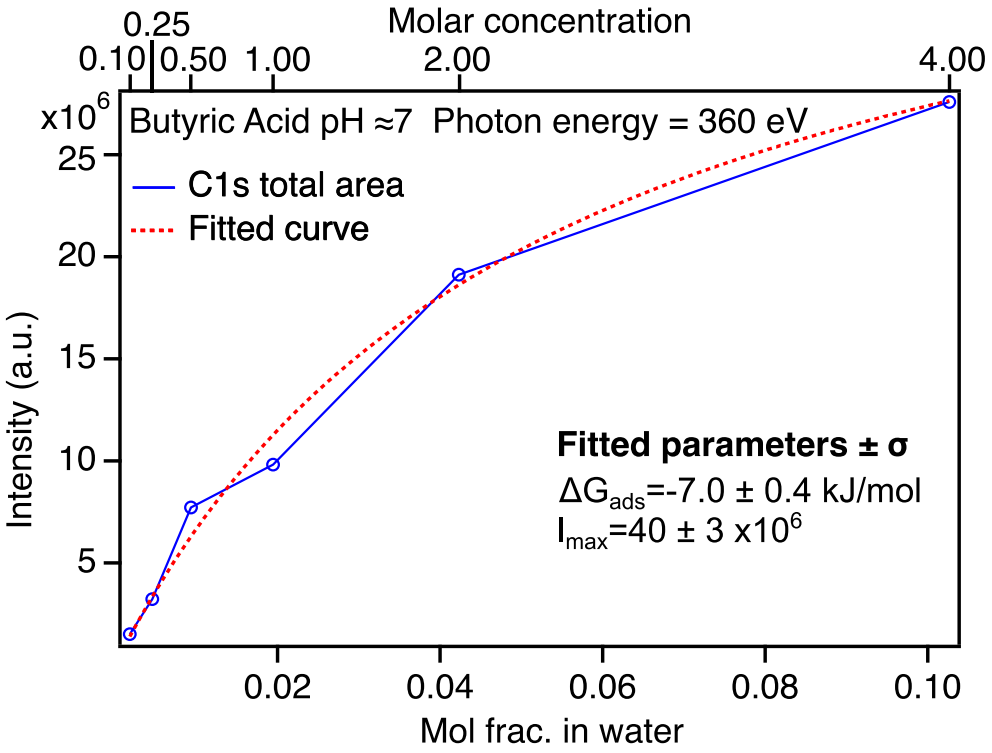

Figure 02: Butyric Acid C 1s total area at different concentrations at pH ≈ 7 and the fitted modified Langmuir curve as hatched line. The optimized fitted parameters are also presented. See text for more details.

The curve depicted in Figure 1 was obtained by applying a least-squares method. Furthermore, we present the optimized fitted parameters. By utilizing these fitted parameters, we calculated the butylamine molar fraction (molar concentration) at $\frac{I_{max}}{2}$ to be 0.0132 (0.7 M). Employing this concentration ensured the liquid surface remained well below saturation at a pH of 7. It is essential to underscore that the surface coverage achieved at the previously mentioned concentrations is relevant at a pH of seven and within a pure butylamine solution.

A similar series of measurements was conducted for butyric acid (BUT). Fig. 2 presents the experimental C 1s total areas for surface-representative photoelectrons ionized by a 360 eV photon. It also illustrates the fitted modified Langmuir curve.

Based on the established parameters and the identical criteria employed for the BAM, we determined the molar fraction (molar concentration) for the BUT sample $\frac{I_{max}}{2}$ to be 00477 (2.0 M) at neutral pH. We have also calculated the surface tension in the same way as we calculated for BAM, obtaining:

$\gamma = 33 \pm 2\ mN/m$ (3).

In the calculation, we used $A_m \approx 0.35\ nm^2$ [7, 10]. The above value can be compared with direct experimental measurements of the surface tension for butyric acid (or its aqueous solutions at pH 7), which typically report values in the $30–35\ mN/m$ range [11 7].

The C 1s intensities of pure BAM and BUT exhibit remarkable similarity at pH 7, as illustrated in Figure 4 (main text). This observation suggests that the surface-sensitive X-ray photoelectron spectroscopy (XPS) measurements detect approximately equal quantities of BAM and BUT molecules, consistent with the aforementioned Langmuir procedure.

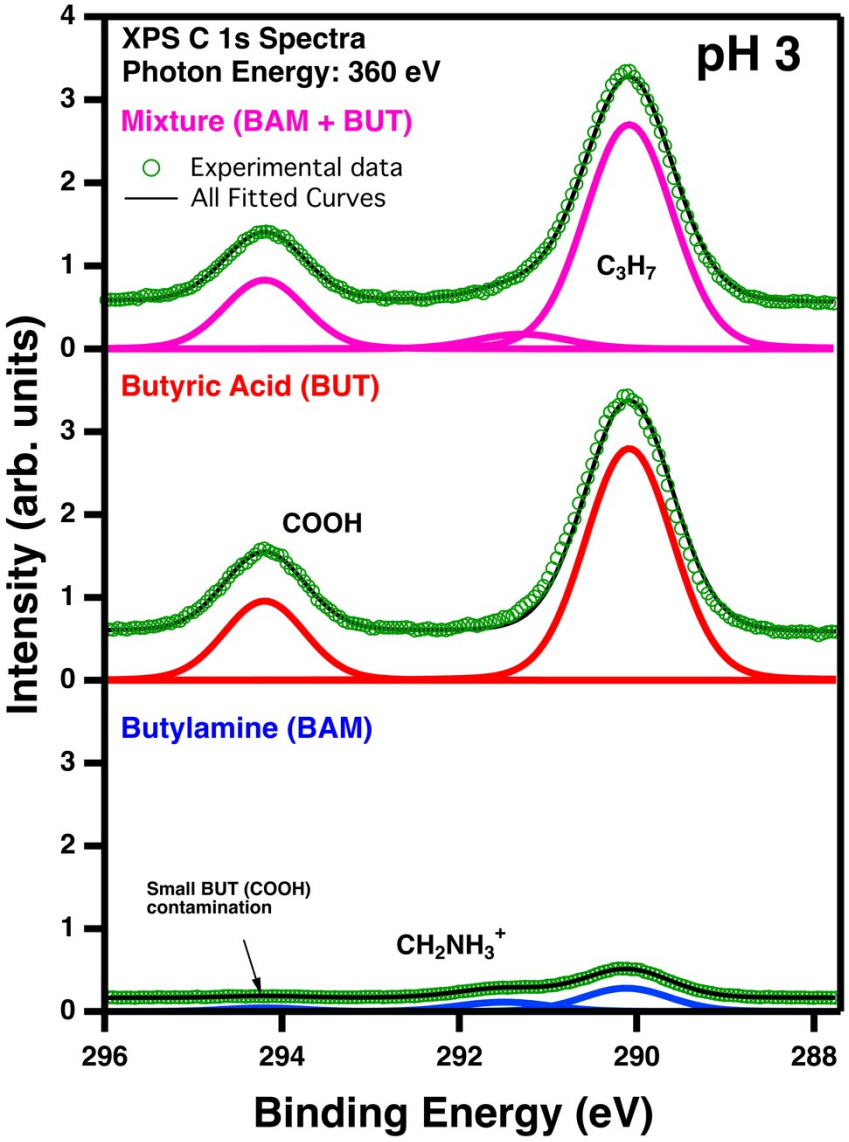

Figure 3: XPS C 1s spectra, recorded with 380 eV of 2.0 M BUT @ pH 2.41, 0.7 M BAM @ pH 2.88, and their mixtures @ pH 3. The species of each spectrum are presented in the figure. The BAM spectrum at pH 3 shows less than 5% contamination of BUT.

7.2. Additional Core level spectra

In Fig. 3, we present the X-ray Photoelectron Spectroscopy C 1s spectra, which were recorded at an energy of 380 eV for a 2.0 M BUT solution at a pH of 2.41, a 0.7 M BAM solution at a pH of 2.88, as well as their mixtures at a pH of 3. The chemically shifted carbon groups in each spectrum are indicated. The BAM spectrum at the bottom of Fig. 3 reveals traces of the carboxylic acid (COOH) species (294.2 eV), representing minor contamination from the BUT

sample remaining in the inlet system. The contamination from the BUT sample has been meticulously accounted for in fitting the BAM spectra.

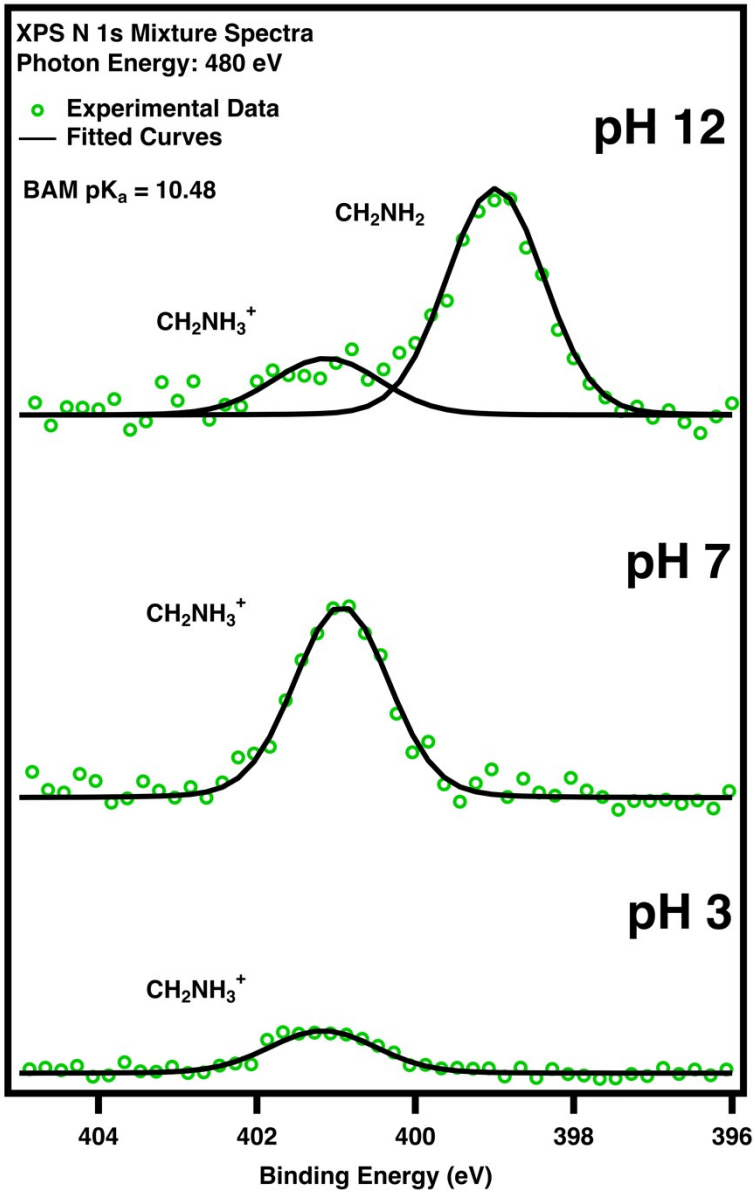

Figure 4: XPS N 1s spectra, measured at 480 eV of 0.7 M BAM at pH 3, 7, and 12.

In Fig. 4, the pK_a of BAM is noted to be 10.48. This indicates the presence of the protonated form (BAM^+) and the neutral form (BAM) at pH values below 12. At pH levels of 3 and 7, the binding energies of N 1s are observed to be greater than those at pH 12 due to the presence of charged species at pH values below the pK_a. At pH 12, a contribution from BAM^+ has been observed; this peak accounts for approximately 27% of neutral BAM. The presence of new species at the solution surface absent from the bulk has been pointed out previously for cysteine [12, 13]. To enhance visualization, the step energies of the spectra were mathematically increased to 100 meV, as opposed to the previous 50 meV configuration. All the relevant fitted parameters are presented in Tab. 1.

Table 1
The fitted spectra' binding energy, area, uncertainties, and Full Width at Half Maximum (FWHM) are presented herein.

Label	BE (eV)	Area	Area Error (%)	FWHM (eV)
Mix N1s @ pH 3				
$CH_2NH_3^+$	401.17	116	14	1.55
Mix N1s @ pH 7				
$CH_2NH_3^+$	400.93	456	6	1.35
Mix N1s @ pH 12				
CH_2NH_2	398.97	574	4	1.43
$CH_2NH_3^+$	401.11	156	6	1.55
Butylamine C1s @ pH 3				
$CH_3CH_2CH_2$	290.12	14589	1	1.14
$CH_2NH_3^+$	291.50	6274	2	1.23
$\boldsymbol{CH_3CH_2CH_2}$	290.08	3253	1	1.16

(BUT Cont.)				
COOH (BUT Cont.)	294.20	1026	7	1.07
Butyric Acid C1s @ pH 3				
$CH_3CH_2CH_2$	290.08	71445	1	1.16
COOH	294.20	22524	2	1.07
Mix C1s @ pH 3				
$CH_3CH_2CH_2$	290.08	68967	2	1.16
$CH_2NH_3^+$	291.30	4785	11	1.23
COOH	294.20	19542	2	1.07
Butylamine C1s @ pH 7				
$CH_3CH_2CH_2$	290.27	11904	2	1.14
$CH_2NH_3^+$	291.68	4875	4	1.25
Butyric Acid C1s @ pH 7				
$CH_3CH_2CH_2$	289.83	23519	2	1.16

COO^-	293.10	4840	2	0.92
COOH	294.06	2186	6	1.18
Mix C 1s @ pH 7				
$CH_3CH_2CH_2$	290.03	56499	1	1.11
$CH_2NH_3^+$	291.38	9817	3	1.20
COO^-	293.22	9169	2	1.10
COOH	294.20	1479	7	1.03
Butylamine C1s @ pH 12				
$CH_3CH_2CH_2$	290.11	38113	1	1.13
CH_2NH_2	290.96	12909	2	1.21
Butyric Acid C1s @ pH 12				
$CH_3CH_2CH_2$	289.92	21441	3	1.16
COO^-	293.28	5363	4	0.87
COOH	294.19	801	6	0.92

Mix C1s @ pH 12				
$CH_3CH_2CH_2$	290.09	49209	2	1.13
CH_2NH_2	290.94	13435	3	1.21
COO^-	293.24	4802	6	0.87
COOH	294.15	873	4	0.92

7.3 Normalization and energy calibration procedures

The storage ring of the LNLS synchrotron accelerator operated in decay mode, resulting in a decrease in photon flux as a function of time following each injection, which occurred every twelve hours. This study conducts a comparison of the intensities of BUT, BAM, and their mixtures as a function of pH by monitoring the area of the C 1s (and N 1s) peaks for each species. Consequently, it is essential to monitor the photon flux that reaches the samples. During the measurements, we did not track the available photon flux, as this parameter is inadequate for conducting an accurate normalization due to potential slight variations in the overlap between the micro-jet beam and the X-ray. To address this issue, we normalized the spectra by utilizing data from the Valence Band (VB) of liquid conductive water. The VB measurements were carried out by introducing conductive water both prior to and following each series of samples. By 'series,' we refer to the X-ray Photoelectron Spectroscopy (XPS) C 1s measurements of the samples at pH levels of 3, 7, and 12. We characterize liquid conductive water as pure water with a minimal concentration of KCl (50 millimolar) to enhance conductivity, thereby making the solution suitable for photoelectron experiments. A similar procedure was described in the Electronic Supplementary Material (ESI) of reference [14]. In the subsequent paragraphs, conductive water will be referred to simply as water in order to minimize redundancy.

The normalization process of the XPS C 1s spectra considers the (fitted area) of $1b_1$ liquid water ($1b_1$_liq) valence band (VB) recorded before and after each C 1s sample's spectra. The $1b_1$_liq areas are represented by the filled circle symbols in Fig. 5, and each sample series is indicated as vertical blue text. The storage ring injections are shown as green vertical bars, and the experimental sections between injections were denoted shift x (x = 1 to 4). A linear regression curve of the $1b_1$_liq area for each shift, as a function of relative time (RT) in seconds, indicates how the storage ring decay mode alters the photon flux and possibly, to a much lesser extent, the interaction between the photon flux and the liquid samples. The horizontal axis represents each measurement's RT, and the first VB spectrum is set as zero seconds. Finally, we can determine the normalization term by using the linear regression of the $1b_1$_liq area as a function of RT. The normalization term for each spectrum is the interpolated point at the same relative time as the C 1s core level measurement. In addition, the normalization procedure considers the number of sweeps (accumulation time).

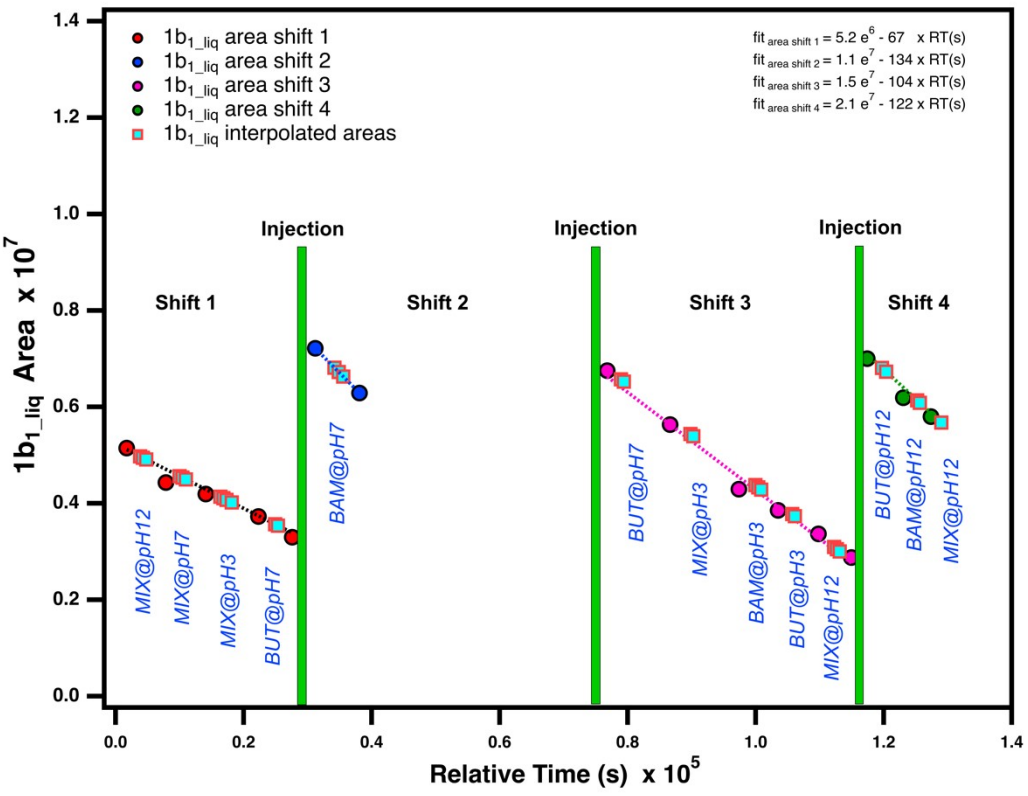

Figure 5: Water $1b_1$_liq VB area (solid circle) as a function of relative time. The normalization term of each spectrum (solid square) is the interpolated point at the same time as the C 1s core level measurement. The green bars represent the electron injection in the LNLS storage ring. Each C 1s core level measurement series, measured between two water valence band spectra, was described in the figure. The interpolation equations for each shift of measurements were indicated in the upper right corner.

7.4 Normalization check for pH 7

We performed a series of tests to verify the quality of the normalization procedure used. Although we present only the verifications for pH 7, the same checks were performed for the spectra at pHs 3 and 12.

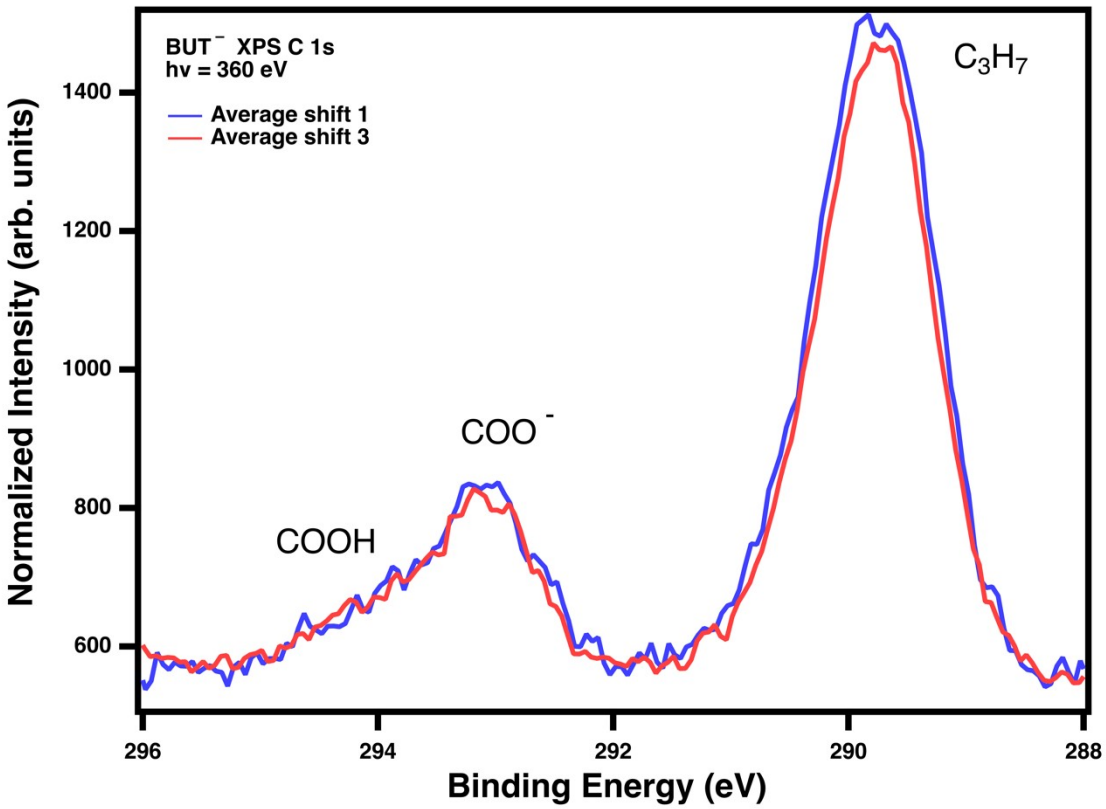

Figure 6: The spectra of BUT^- C 1s measured at shifts 1 and 3 were normalized in accordance with the procedure detailed in session 7.3. The species observed have been labeled within the graph for clarity. The blue solid curve represents the averaged spectrum obtained at shift 1, whereas the red solid line indicates the averaged spectrum at shift 3. The two spectra show a reasonable agreement within the bounds of statistical variation, thereby supporting the findings presented in the main text, which are based on intensity variations significantly larger than the minor uncertainties depicted in this figure.

Fig. 6 shows that the C 1s spectra of the BUT solution at pH seven were recorded at the end of shift one and the beginning of shift three. Therefore, comparing the two normalized spectra reassures us of the quality of the normalization performed in the last session. At a pH higher than the pK_a of BUT (4.82), butyric acid deprotonates, and the COO^- species arise, with binding energy ≈ 293 eV. However, the COOH species can still be observed in the spectrum at a higher binding energy (≈ 294 eV), and the C_3H_7 backbone, the most intense peak, appears at a binding energy of ≈ 290 eV. In Fig. 6, the solid blue and red curves are the average spectra for shifts 1 and 3. The intensities, normalized according to the previous section of the two spectra, are closely aligned, indicating that the normalization procedure is effective.

References

1. I. Langmuir, *J. Am. Chem. Soc.*, 1932, **54**, 2798-2832.
2. M. M. Walz, C. Caleman, J. Werner, V. Ekholm, D. Lundberg, N. L. Prisle, G. Ohrwall and O. Bjorneholm, *Phys. Chem. Chem. Phys.*, 2015, **17**, 14036-14044.
3. R. M. Onorato, D. E. Otten and R. J. Saykally, *Proc. Natl. Acad. Sci. U.S.A.*, 2009, **106**, 15176-15180.
4. K. A. Perrine, M. H. Van Spyk, A. M. Margarella, B. Winter, M. Faubel, H. Bluhm and J. C. Hemminger, *J. Phys. Chem. C*, 2014, **118**, 29378-29388.
5. M. Faubel, in *Photoionization and Photodetachment*, 2000, pp. 634-690.
6. A. W. Adamson and A. P. Gast, *Physical Chemistry of Surfaces*, Interscience publishers New York, 1997.
7. A. W. Adamson and A. P. Gast, *Physical Chemistry of Surfaces*, Interscience publishers New York, 1967.
8. W. M. Haynes, *CRC handbook of chemistry and physics*, CRC press, 2016.
9. M. J. Rosen and J. T. Kunjappu, *Surfactants and interfacial phenomena*, John Wiley & Sons, 2012.
10. J. N. Israelachvili, *Intermolecular and surface forces*, Academic press, 2011.
11. D. R. Lide, *CRC handbook of chemistry and physics*, CRC press, 2004.
12. A. M. da Silva, A. Mocellin, S. Monti, C. Li, R. R. T. Marinho, A. Medina, H. Ågren, V. Carravetta and A. Naves de Brito, *J. Phys. Chem. Lett.*, 2015, **6**, 807-811.
13. O. Björneholm, G. Öhrwall, A. N. de Brito, H. Ågren and V. Carravetta, *Acc. Chem. Res.*, 2022, **55**, 3285-3293.
14. V. Carravetta, A. H. d. A. Gomes, R. d. R. T. Marinho, G. Öhrwall, H. Ågren, O. Björneholm and A. N. de Brito, *Phys. Chem. Chem. Phys.*, 2022, **24**, 26037-26045.